GEOPHYSICAL RESEARCH LETTERS, VOL. 39, L17602, doi:10.1029/2012GL052935, 2012

Weighing the ocean: Using a single mooring to measure changes in the mass of the ocean

Chris W. Hughes,[1] Mark E. Tamisiea,[1] Rory J. Bingham,[2] and Joanne Williams[1]

Received 1 July 2012; accepted 21 July 2012; published 1 September 2012.

[1] Combining ocean and earth models, we show that there is a region in the central Pacific ocean where ocean bottom pressure is a direct measure of interannual changes in ocean mass, with a noise level for annual means below 3 mm water equivalent, and a trend error below 1 mm/yr. We demonstrate this concept using existing ocean bottom pressure measurements from the region, from which we extract the annual cycle of ocean mass (amplitude 8.5 mm, peaking in late September), which is in agreement with previous determinations based on complex combinations of global data sets. This method sidesteps a number of limitations in satellite gravity-based calculations, but its direct implementation is currently limited by the precision of pressure sensors, which suffer from significant drift. Development of a low-drift method to measure ocean bottom pressure at a few sites could provide an important geodetic constraint on the earth system. **Citation:** Hughes, C. W., M. E. Tamisiea, R. J. Bingham, and J. Williams (2012), Weighing the ocean: Using a single mooring to measure changes in the mass of the ocean, *Geophys. Res. Lett.*, *39*, L17602, doi:10.1029/2012GL052935.

1. Introduction

[2] The GRACE satellite gravity mission has revolutionized our ability to monitor regional mass redistribution in the earth system, and hence monitor changes in ocean mass and the source of those changes. However, GRACE does not monitor the degree 1 terms in mass movement, associated with geocenter motion, and is weak for the $C_{2,0}$ harmonic [*Chen et al.*, 2006; *Swenson et al.*, 2008; *Leuliette and Miller*, 2009]. It also suffers from limited spatial resolution, making it hard to distinguish the much larger land signals from ocean signals near the ocean boundaries [*Chambers et al.*, 2007], and secular trends include a contribution from glacial isostatic adjustment (GIA), the solid earth's ongoing response to the change in load since the last glaciations [*Tamisiea*, 2011]. Together, these difficulties lead to an uncertainty approaching 1 mm/yr in the measured mass component of global sea level trend.

[3] If sea level changes were spatially uniform, then variation of the volume of the ocean could be monitored using a single tide gauge. Similarly, spatially uniform changes in ocean bottom pressure (OBP) would mean ocean mass changes could be monitored with a single OBP Recorder. However, spatial variations mean that sea level measurements must be made over the entire ocean (by satellite altimetry), or statistical extrapolation must be used to mitigate the sampling problems of tide gauge data [*Hughes and Williams*, 2010; *Church and White*, 2006; *Jevrejeva et al.*, 2006]. Fortunately, as we will show, OBP observations in one specific region do allow us to measure ocean mass changes with a single station.

2. Model Predictions

[4] The effect of a sloping sea floor means that there are much stronger dynamical constraints on OBP than on sea level [*Hughes and de Cuevas*, 2001]. This means that OBP variations tend to be smaller in amplitude and have larger spatial scales than sea level variations [*Vinogradova et al.*, 2007; *Bingham and Hughes*, 2008]. The dynamical constraint has the largest effect near the equator. Here, the strong stratification and rapid propagation of Rossby waves mean that wind-driven flows tend to be limited to a shallow surface layer. As any deeper circulation approaches the equator, geostrophic balance results in smaller pressure differences for a given mass transport. Power spectra of dynamical OBP (i.e. with the global average subtracted at each time), based on 19 years of data from three different ocean models (OCC12: the 1/12° resolution OCCAM model [*Marsh et al.*, 2009]; the 18 km resolution ECCO2 model from Jet Propulsion Laboratory [*Menemenlis et al.*, 2005]; and OCC4: run 202 of the 1/4° OCCAM model [*Marsh et al.*, 2008]) illustrate how strong this dynamical suppression of OBP variability is (Figure 1). Tropical Pacific OBP variability in the deep ocean has 500–1000 times less power than typical sea level variability at interannual time scales.

[5] For a running annual mean of OBP, this spectrum translates into a standard deviation of less than 3 mm of water in the tropical Pacific (Figure 2a and Figures S1 and S2 in the auxiliary material).[1] A Monte Carlo simulation based on the spectrum in Figure 1a predicts that 95% of trends will be less than 0.85 mm/yr when calculated over 5-year periods, and less than 0.28 mm/yr over 10-year periods. Current estimates for the recent rate of sea level rise due to ocean mass increase are about 1–2 mm/year, with much of the uncertainty accounted for by differences in GIA models [*Tamisiea*, 2011; *Cazenave and Llovel*, 2010; *Chambers et al.*, 2010; *Riva et al.*, 2010], so the errors from a ten-year OBP record would be only a small fraction of the estimated trend.

[6] All three models exhibit realistic variability in Tropical Pacific sea level (Figure S3 in the auxiliary material), but we

[1]National Oceanography Centre, Liverpool, UK.
[2]School of Civil Engineering and Geosciences, Newcastle University, Newcastle upon Tyne, UK.

Corresponding author: C. W. Hughes, National Oceanography Centre, Joseph Proudman Bldg., 6 Brownlow St., Liverpool L3 5DA, UK. (cwh@noc.ac.uk)

0094-8276/12/2012GL052935

[1]Auxiliary materials are available in the HTML. doi:10.1029/2012GL052935.

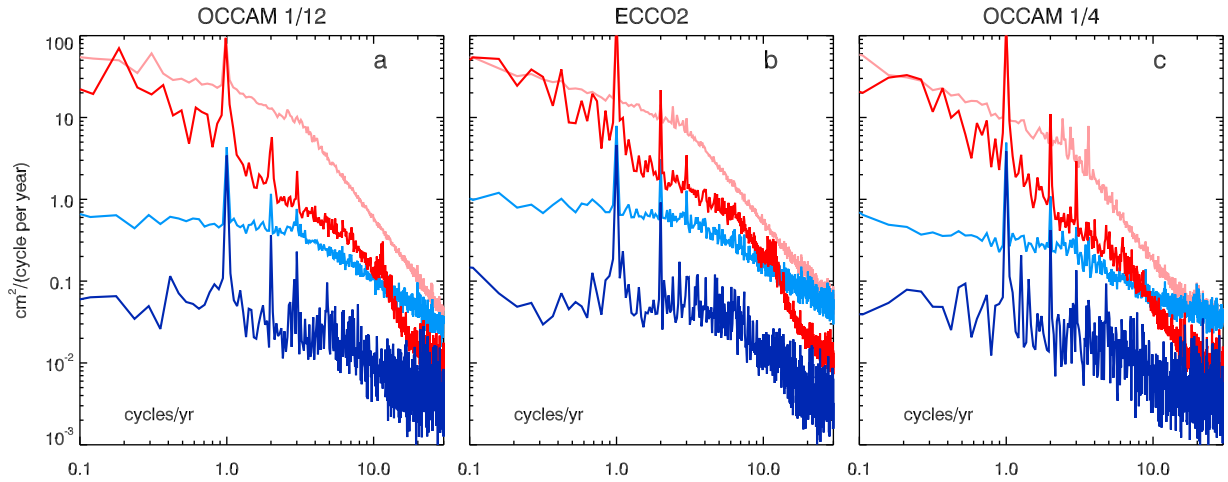

Figure 1. Power spectral density of sea level (red) and ocean bottom pressure (blue, in equivalent cm of water) for ocean regions deeper than 3000 m. Dark colors represent the Pacific Ocean between 15°S and 15°N. Pale colors represent all areas between latitudes 15 and 65 degrees north and south. Spectra are calculated by area-weighted averaging of periodograms from each grid point in the region, from three different ocean models: (a) the 1/12° resolution OCCAM model, (b) the 18 km resolution ECCO2 model, and (c) run 202 of the 1/4° OCCAM model.

expect model trends to be larger than real world trends: unrealistically large transient thermohaline adjustment processes, lasting for several decades, occur even in relatively coarse resolution models for which a flux adjustment can be estimated to minimize shocks [*Collins et al.*, 2006]. Figure 2b shows that the model OBP trends are, as expected, larger than our statistical estimate, particularly in the Atlantic and Southern oceans where deep water mass formation is important. Nonetheless, most of the Pacific shows trends below 1 mm/yr even with this unrealistically large adjustment process taking place, suggesting that the statistical uncertainty estimate of 0.28 mm/yr is probably not far from the true dynamical OBP trend. The dynamical signal is therefore small enough that a measurement of secular OBP trend at a single point could provide a valuable constraint on the secular increase in ocean mass.

[7] Even in the absence of ocean dynamics, there are other causes of spatially non-uniform OBP change. The effects of long period tidal forcing and earth rotation changes (the pole tide) are well understood and straightforward to remove from measurements [*Woodworth*, 2012; *Desai*, 2002], as is the variation in the average pressure exerted by the atmosphere on the ocean. More difficult to model and remove is the effect of flexing of the earth under changing loads, and related changes to the gravity field, which lead to a redistribution of water. For example, if Greenland ice melts and increases the mass of the ocean, the resulting local OBP signal is equal to the global average signal multiplied by an amplification factor which is actually negative within about 2500 km of Greenland, and a little larger than one in the far field [*Clark and Primus*, 1987; *Mitrovica et al.*, 2001]. For most ocean sites, this means that the pressure signal resulting from far-field sources of water can be offset by that from nearby sources; only at sites far from all land is the bottom pressure change insensitive to the position of the source.

[8] To investigate this effect, we split the continents into 2283 regions of similar area, and calculated the consequences of transferring a standard mass of water into the ocean, from any one of these regions. For each region, the resulting gravitationally self-consistent equilibrium distribution of water was calculated, accounting for loading and self attraction effects but ignoring feedbacks due to changes in earth rotation [*Tamisiea et al.*, 2010], followed by a 50 km Gaussian smoothing. This gave 2283 OBP predictions at each ocean point, each one representing the response to a different water source region. The contours in Figure 2 show the ratio of the smallest to the largest of these values, at each point, with numbers close to 1 indicating that the response at that point is insensitive to where on land the additional water originated from.

[9] Negative values of this ratio (not plotted), indicate that mass loss from some land regions would reduce OBP at those points. There is, however, a large region in the Pacific where all land sources contribute positively to OBP. The ratio reaches a maximum of 0.785, meaning there are locations where OBP responds to mass changes from all land regions with almost the same relative weighting. In this region, OBP is a direct measure of ocean mass change almost independent of the source location.

[10] In addition to this elastic earth response to loading, we must also consider the long-term viscoelastic signal which is dominated by GIA. This contributes a significant component (of order 0.5 mm/yr) to the uncertainty in ocean mass trend estimates from satellite gravity data [*Cazenave and Llovel*, 2010; *Chambers et al.*, 2010; *Tamisiea*, 2011]. However, the high density of rock relative to water means that this solid earth effect is proportionately larger in gravity measurements than in OBP. Using data from *Tamisiea* [2011], we find at Sites S and N (Figure 2), a GIA contribution to OBP variation of −0.15 mm/yr when using the ICE-5G ice history (halting ice sheet variations at 4000 years before present), and the VM2 earth model [*Peltier*, 2004]. Alternatively, using the older ICE-3G model and its corresponding earth model [*Tushingham and Peltier*, 1991] we obtain −0.16 mm/yr at site S and −0.17 mm/yr at site N. Varying the earth model parameters over the range explored in *Tamisiea* [2011], without varying the ice model so as to be consistent with observations, leads to an overestimate of the possible

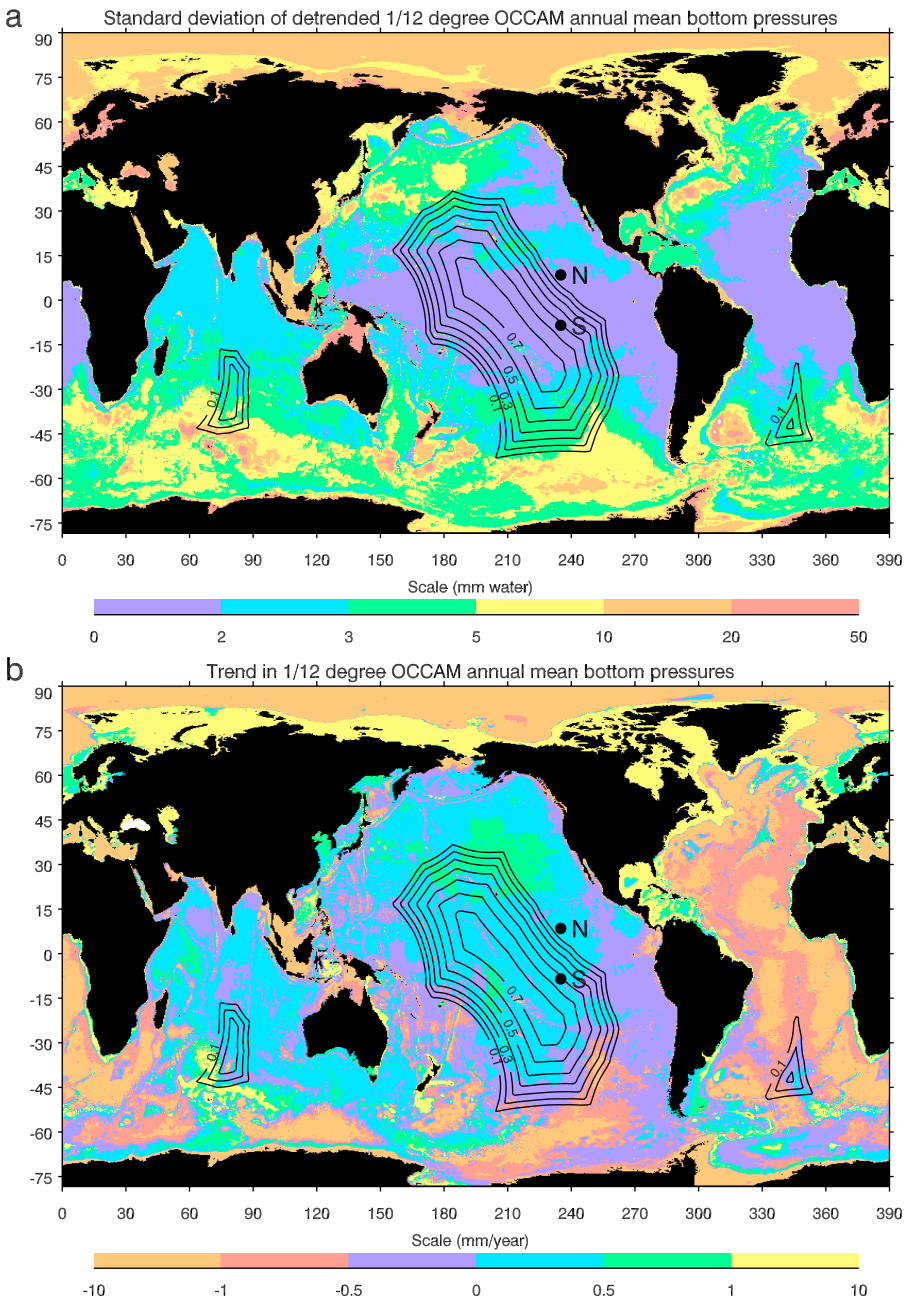

Figure 2. Ocean Bottom Pressure diagnostics from 19 years of data from the 1/12° resolution OCCAM ocean model: (a) standard deviation of the running-annual-average, detrended time series and (b) the linear trend in the time series. Each panel also shows the positions, sites N and S, of two deployed OBP recorders. Contours show the ratio of minimum to maximum amplification factor for OBP signals resulting from moving a standard mass from any land point to its equilibrium configuration in the ocean.

variation in this signal. This produces an extreme range of −0.55 to +0.01 mm/yr at site S, and from −0.31 to +0.19 mm/yr at site N, to be compared with the equivalent extreme range of GIA contributions to the GRACE measurement of −1.9 to −0.5 mm/yr.

[11] Taken together, these results indicate that OBP variations in a region of the central tropical Pacific ocean reflect ocean mass changes (multiplied by an amplification factor of about 1.16), with relatively little noise resulting from ocean dynamics or solid earth processes. The noise amounts to less than 3 mm standard error for annual means, and less (probably much less) than 1 mm/yr in 10-year trends.

3. Mass Measurement

[12] We wish to demonstrate that a single OBP time series can, in practice, measure ocean mass changes. However, present limitations of in-situ OBP recorders mean that we cannot directly measure long-term trends to the accuracy required. In fact the longest-period signal which can be

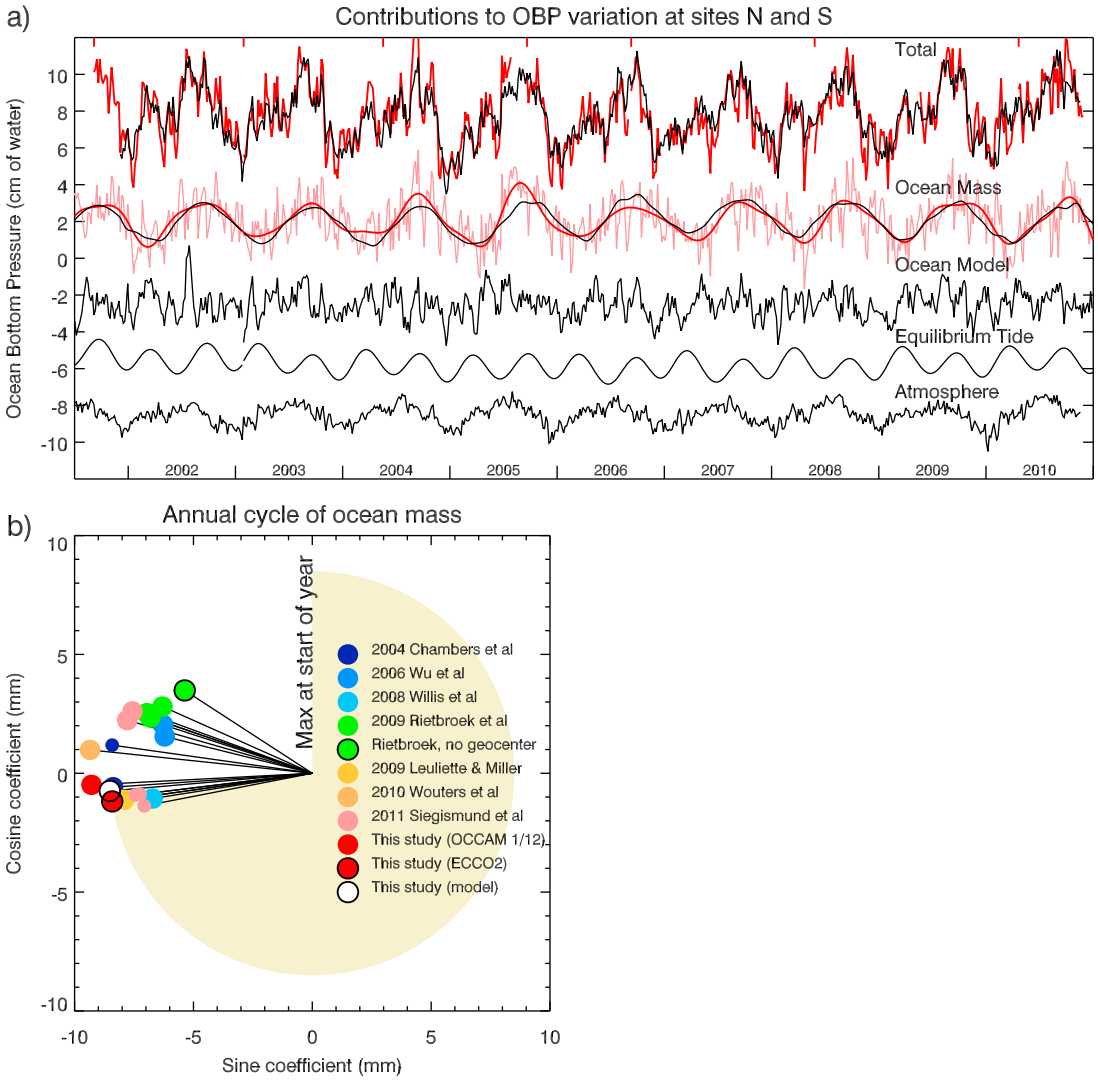

Figure 3. (a) Modeled (black) and measured (red) time series of OBP, and the individual contributions to OBP, from sites N and S in the tropical Pacific. The start of each instrument deployment is marked with a red tick at the top, the first deployment being at N and all others at S. The ocean mass term is shown as modeled (black), and also as calculated from a residual of the measured OBP minus all other modeled terms, both before (pale red) and after (dark red) applying a 5-month low pass filter. (b) Phasor diagram showing the annual cycles of ocean mass as calculated in this study, and by other authors using global satellite data sets. Time of year of the maximum in ocean mass should be read clockwise from the start of January at the top of the plot. Amplitude is in equivalent global-ocean-average millimetres of water.

measured is comparable to the length of individual instrument deployments, typically a year [*Watts and Kontoyiannis*, 1990]. Satellite-based determinations of ocean mass changes [e.g., *Willis et al.*, 2008] show that the signal is dominated by an annual cycle and longer-period variability. If we are to use available data to test whether this concept works in practice, we must therefore focus on the annual cycle.

[13] Fortuitously, as part of the US National Tsunami Hazard Mitigation Program [*Gonzalez et al.*, 2005] OBP measurements have been made at site N (125.0°W, 8.5°N, station number 50184) in 2001–2002, and then at site S (125.0°W, 8.5°S, station number 51406) since 2002. Following subtraction by least squares fitting of tides with periods of 1 month and shorter, and correction from sensor drift using the standard exponential-plus-linear drift formula of *Watts and Kontoyiannis* [1990] (discussed in more detail below), a time series of 5-day means of OBP anomaly is produced, plotted in Figure 3a (top red curve).

[14] Figure 3a also shows (black lines) the predicted contribution to this OBP signal from a set of independent models. The ocean mass contribution is modeled using a combination of hydrological and atmospheric model data with satellite gravity data for the cryosphere [*Tamisiea et al.*, 2010]. The dynamical ocean signal is from the ECCO2 model (OCC12 produces very similar results, but ends at the start of 2007; OCC4 ends at the start of 2003). The equilibrium tide includes all gravitational terms longer than a month and a self-consistent treatment of loading and self-attraction as in *Woodworth* [2012]. It also includes the pole tide using a similar treatment due to *Desai* [2002], and the EOP 08 C04 data set of earth orientation parameters,

from the International Earth Rotation and Reference System Service at http://www.iers.org, with a 35-day low-pass filter applied (dominant periods are annual and 433 days). The atmospheric pressure averaged over the global ocean is from the ECMWF analysis data set provided as a satellite altimeter product by AVISO.

[15] The sum of all predicted contributions explains 73% of the observed signal variance. The ocean model alone explains 33%, while the sum of all other contributions explains 53%, showing that the ocean dynamical contribution is far from dominating the signal. Figure 3a also shows the ocean mass derived by subtracting all other modeled contributions from the observations. After applying a 5-month low pass filter, this agrees well with the modeled ocean mass, which is dominated by an annual signal.

[16] The instrumental drift removal procedure, coupled with the typically 1–2 year deployment lengths, means that the annual cycle is the longest period signal which can be meaningfully extracted from the data. Even this requires careful analysis, as the drift removal will tend to absorb some of the true signal and hence reduce the amplitude of the annual cycle. We avoid this, while maintaining independence of the annual mass signal determination, by implementing an iterative drift removal. We make a prediction of the total signal by summing all the model contributions, but representing the mass contribution only by an arbitrary annual cycle. This model is subtracted from the data, and the drift function is fitted to the residual. After drift removal, there should be no annual cycle in the residual if the assumed mass signal is correct. An annual cycle correction to the mass model is then calculated from an annual fit to the dedrifted residual, and the procedure iterated until the annual cycle becomes self-consistent. The procedure converges rapidly to a single result, independent of starting conditions. After dividing by the amplification factor appropriate to this signal (1.17 at site S), this produces an annual cycle of ocean mass with amplitude 8.5 mm, phase 262° (a phase of zero represents an annual peak at the start of the year, so this corresponds to a maximum in late September).

[17] If, instead, of ECCO2, we use OCC12, this becomes 9.3 mm and 267°. OCC4 has too little overlap with the data for a complete calculation, but has a similar annual cycle: (OCC4, OCC12, ECCO2) annual cycles at site S have amplitudes of (4.5, 5.6, 4.7) mm and phases of (180, 171, 173) degrees respectively. Uncertainties in the other OBP contributions are much smaller than this, making ocean model skill the limiting factor, and suggesting an error in the ocean mass annual cycle with amplitude about 1 mm.

[18] In Figure 3b we compare the annual cycle of ocean mass derived using (effectively) a single OBP recorder, to that determined from global satellite and in-situ data sets [*Chambers et al.*, 2004; *Wu et al.*, 2006; *Willis et al.*, 2008; *Rietbroek et al.*, 2009; *Leuliette and Miller*, 2009; *Wouters et al.*, 2011; *Siegismund et al.*, 2011]. The results are consistent, and the scatter introduced by ocean model uncertainty is smaller than the scatter among different determinations using global data sets.

4. Discussion and Conclusions

[19] We have shown that the quiet environment and large distance from land in the central Pacific ocean make it possible to use a single OBP recorder to determine the annual cycle of ocean mass at least as well as can be achieved using global satellite and in-situ data sets. If the model predictions remain correct at longer time scales, a tropical Pacific OBP measurement on its own would provide an ocean mass monitoring system capable of resolving trends as small as 1 mm/yr, and probably significantly less. However, it is probably better to consider such a measurement in combination with a satellite gravity monitoring system like GRACE. A small network of tropical OBP measurements would provide a tie between satellite and in-situ measurements, analogous to the vital role played by tide gauges in maintaining the calibration of satellite altimeter measurements [*Leuliette et al.*, 2004]. Such measurements would help to address the uncertainties due to GIA and poorly-measured low spherical harmonic degrees of the mass redistribution, and hence would contribute to the accuracy of the International Terrestrial Reference Frame (ITRF) as a whole, with benefits to a wide range of satellite-based geophysical measurements. Satellite and in-situ measurements would mitigate each other's limitations, providing better measurements than either would be capable of alone.

[20] Measurement of secular changes in ocean mass would require an OBP measurement system which can operate in depths of 4–5 km, with long-term drift of a fraction of a millimetre (a few pascal) per year. Instruments capable of achieving this stability currently do not exist, but their development would lead to an important constraint on the earth system from just a small number of instruments; as we have shown, even present-day instruments can provide such a constraint at the annual period. An alternative method would combine detailed sea level and density measurements to infer bottom pressure, though the sampling and stability requirements remain challenging.

[21] **Acknowledgments.** We thank the OCCAM team for making the model data available, Philip Woodworth and Ian Vassie for their help, and NOAA National Data Buoy Center for the OBP data. The ECCO2 state estimates were provided by the ECCO Consortium for Estimating the Circulation and Climate of the Ocean funded by the National Oceanographic Partnership Program (NOPP). ECMWF atmospheric pressure, and altimetry produced by Ssalto/Duacs, were distributed by Aviso, with support from CNES. The work was funded by the UK Natural Environment Research Council through National Capability funding and grant NE/1023384/1.

[22] The Editor thanks two anonymous reviewers for their assistance in evaluating this paper.

References

Bingham, R. J., and C. W. Hughes (2008), The relationship between sea-level and bottom pressure variability in an eddy permitting ocean model, *Geophys. Res. Lett.*, *35*, L03602, doi:10.1029/2007GL032662.

Cazenave, A., and W. Llovel (2010), Contemporary sea level rise, *Annu. Rev. Mar. Sci.*, *2*, 145–173, doi:10.1146/annurev-marine-120308-081105.

Chambers, D. P., J. Wahr, and R. S. Nerem (2004), Preliminary observations of global ocean mass variations with GRACE, *Geophys. Res. Lett.*, *31*, L13310, doi:10.1029/2004GL020461.

Chambers, D. P., M. E. Tamisiea, R. S. Nerem, and J. C. Ries (2007), Effects of ice melting on GRACE observations of ocean mass trends, *Geophys. Res. Lett.*, *34*, L05610, doi:10.1029/2006GL029171.

Chambers, D. P., J. Wahr, M. E. Tamisiea, and R. S. Nerem (2010), Ocean mass from GRACE and glacial isostatic adjustment, *J. Geophys. Res.*, *115*, B11415, doi:10.1029/2010JB007530.

Chen, J. L., C. R. Wilson, and K.-W. Seo (2006), Optimized smoothing of Gravity Recovery and Climate Experiment (GRACE) time-variable gravity observations, *J. Geophys. Res.*, *111*, B06408, doi:10.1029/2005JB004064.

Church, J. A., and N. J. White (2006), A 20th century acceleration in global sea-level rise, *Geophys. Res. Lett.*, *33*, L01602, doi:10.1029/2005GL024826.

Clark, J. A., and J. A. Primus (1987), Sea-level changes resulting from future retreat of ice sheets: An effect of CO_2 warming of the climate, in

Sea-Level Changes, *IBG Spec. Publ. Ser.*, vol. 20, edited by M. J. Tooley and I. Shennan, pp. 356–370, Blackwell, Oxford, U. K.

Collins, M., B. B. B. Booth, G. R. Harris, J. M. Murphy, D. M. H. Sexton, and M. J. Webb (2006), Towards quantifying uncertainty in transient climate change, *Clim. Dyn.*, *27*(2–3), 127–147, doi:10.1007/s00382-006-0121-0.

Desai, S. D. (2002), Observing the pole tide with satellite altimetry, *J. Geophys. Res.*, *107*(C11), 3186, doi:10.1029/2001JC001224.

Gonzalez, F., E. Bernard, C. Meinig, M. Eble, H. Mofjeld, and S. Stalin (2005), The NTHMP tsunameter network, *Nat. Hazards*, *35*(1), 25–39.

Hughes, C. W., and B. A. de Cuevas (2001), Why western boundary currents in realistic oceans are inviscid: A link between form stress and bottom pressure torques, *J. Phys. Oceanogr.*, *31*(10), 2871–2885.

Hughes, C. W., and S. D. P. Williams (2010), The color of sea level: Importance of spatial variations in spectral shape for assessing the significance of trends, *J. Geophys. Res.*, *115*, C10048, doi:10.1029/2010JC006102.

Jevrejeva, S., A. Grinsted, J. C. Moore, and S. Holgate (2006), Nonlinear trends and multiyear cycles in sea level records, *J. Geophys. Res.*, *111*, C09012, doi:10.1029/2005JC003229.

Leuliette, E. W., and L. Miller (2009), Closing the sea level rise budget with altimetry, Argo, and GRACE, *Geophys. Res. Lett.*, *36*, L04608, doi:10.1029/2008GL036010.

Leuliette, E. W., R. S. Nerem, and G. T. Mitchum (2004), Calibration of TOPEX/Poseidon and Jason altimeter data to construct a continuous record of mean sea level change, *Mar. Geod.*, *27*(1–2), 79–94, doi:10.1080/01490410490465193.

Marsh, R., S. A. Josey, B. A. de Cuevas, L. J. Redbourn, and G. D. Quartly (2008), Mechanisms for recent warming of the North Atlantic: Insights gained with an eddy-permitting model, *J. Geophys. Res.*, *113*, C04031, doi:10.1029/2007JC004096.

Marsh, R., B. A. de Cuevas, A. C. Coward, J. Jacquin, J. J. M. Hirschi, Y. Aksenov, A. J. G. Nurser, and S. A. Josey (2009), Recent changes in the North Atlantic circulation simulated with eddy-permitting and eddy-resolving ocean models, *Ocean Modell.*, *28*(4), 226–239, doi:10.1016/j.ocemod.2009.02.007.

Menemenlis, D., I. Fukumori, and T. Lee (2005), Using Green's functions to calibrate an ocean general circulation model, *Mon. Weather Rev.*, *133*(5), 1224–1240, doi:10.1175/MWR2912.1.

Mitrovica, J. X., M. E. Tamisiea, J. L. Davis, and G. A. Milne (2001), Recent mass balance of polar ice sheets inferred from patterns of global sea-level change, *Nature*, *409*(6823), 1026–1029.

Peltier, W. (2004), Global glacial isostasy and the surface of the ice-age Earth: The ICE-5G (VM2) model and GRACE, *Annu. Rev. Earth Planet. Sci.*, *32*(1), 111–149, doi:10.1146/annurev.earth.32.082503.144359.

Rietbroek, R., S.-E. Brunnabend, C. Dahle, J. Kusche, F. Flechtner, J. Schröter, and R. Timmermann (2009), Changes in total ocean mass derived from GRACE, GPS, and ocean modeling with weekly resolution, *J. Geophys. Res.*, *114*, C11004, doi:10.1029/2009JC005449.

Riva, R. E. M., J. L. Bamber, D. A. Lavallée, and B. Wouters (2010), Sea-level fingerprint of continental water and ice mass change from GRACE, *Geophys. Res. Lett.*, *37*, L19605, doi:10.1029/2010GL044770.

Siegismund, F., V. Romanova, A. Köhl, and D. Stammer (2011), Ocean bottom pressure variations estimated from gravity, nonsteric sea surface height and hydrodynamic model simulations, *J. Geophys. Res.*, *116*, C07021, doi:10.1029/2010JC006727.

Swenson, S., D. Chambers, and J. Wahr (2008), Estimating geocenter variations from a combination of GRACE and ocean model output, *J. Geophys. Res.*, *113*, B08410, doi:10.1029/2007JB005338.

Tamisiea, M. E. (2011), Ongoing glacial isostatic contributions to observations of sea level change, *Geophys. J. Int.*, *186*(3), 1036–1044, doi:10.1111/j.1365-246X.2011.05116.x.

Tamisiea, M. E., E. M. Hill, R. M. Ponte, J. L. Davis, I. Velicogna, and N. T. Vinogradova (2010), Impact of self-attraction and loading on the annual cycle in sea level, *J. Geophys. Res.*, *115*, C07004, doi:10.1029/2009JC005687.

Tushingham, A. M., and W. R. Peltier (1991), Ice-3G: A new global model of late Pleistocene deglaciation based upon geophysical predictions of post-glacial relative sea level change, *J. Geophys. Res.*, *96*(B3), 4497–4523, doi:10.1029/90JB01583.

Vinogradova, N. T., R. M. Ponte, and D. Stammer (2007), Relation between sea level and bottom pressure and the vertical dependence of oceanic variability, *Geophys. Res. Lett.*, *34*, L03608, doi:10.1029/2006GL028588.

Watts, D. R., and H. Kontoyiannis (1990), Deep-ocean bottom pressure measurement: Drift removal and performance, *J. Atmos. Oceanic Technol.*, *7*(2), 296–306, doi:10.1175/1520-0426(1990)007<0296:DOBPMD>2.0.CO;2.

Willis, J. K., D. P. Chambers, and R. S. Nerem (2008), Assessing the globally averaged sea level budget on seasonal to interannual timescales, *J. Geophys. Res.*, *113*, C06015, doi:10.1029/2007JC004517.

Woodworth, P. L. (2012), A note on the nodal tide in sea level records, *J. Coastal Res.*, *28*(2), 316–323, doi:10.2112/JCOASTRES-D-11A-00023.1.

Wouters, B., R. E. M. Riva, D. A. Lavallée, and J. L. Bamber (2011), Seasonal variations in sea level induced by continental water mass: First results from GRACE, *Geophys. Res. Lett.*, *38*, L03303, doi:10.1029/2010GL046128.

Wu, X., M. B. Heflin, E. R. Ivins, and I. Fukumori (2006), Seasonal and interannual global surface mass variations from multisatellite geodetic data, *J. Geophys. Res.*, *111*, B09401, doi:10.1029/2005JB004100.